

# Synthesis of Microporous Inorganic–Organic Hybrids from Layered Octosilicate by Silylation with 1,4-Bis(trichloro- and dichloromethyl-silyl)benzenes

Dai Mochizuki,<sup>†</sup> Sachiko Kowata,<sup>†</sup> and Kazuyuki Kuroda<sup>\*,†,‡,§</sup>

Department of Applied Chemistry, Waseda University, Ohkubo-3, Shinjuku-ku, Tokyo 169-8555, Japan, Kagami Memorial Laboratory for Materials Science and Technology, Waseda University, Nishiwaseda-2, Shinjuku-ku, Tokyo 169-0051, Japan, and CREST, Japan Science and Technology Agency (JST), Japan

Received June 11, 2006. Revised Manuscript Received September 4, 2006

Crystalline microporous inorganic–organic nanohybrids were synthesized by pillaring layered octosilicate with 1,4-bis(trichlorosilyl)benzene or 1,4-bis(dichloromethylsilyl)benzene. The silylating agents were preferentially bridged between the layers of octosilicate, resulting in the formation of microporous hybrids with BET surface areas of  $\sim 500$  m<sup>2</sup>/g. The trichlorosilyl or dichloromethylsilyl groups were regularly grafted with confronting two Si–OH groups on the same octosilicate surface, and each reacted group possessed one unreacted site (chloro or methyl group). The micropores derived from 1,4-bis(trichlorosilyl)benzene showed a hydrophilic nature due to remaining Si–OH groups after hydrolysis of chlorosilyl groups, whereas those derived from 1,4-bis(dichloromethylsilyl)benzene showed a hydrophobic nature. The difference affected the phenol adsorption behavior from dilute aqueous solutions.

## Introduction

Microporous inorganic–organic hybrids with crystalline structures are of great importance as molecular sieves and catalysts.<sup>1–4</sup> Many attempts have been devoted to the development of these new hybrids. Microporous hybrids derived from supramolecular construction of metal coordination polymers are rendered by the spontaneous aggregation of building units.<sup>3</sup> In contrast, microporous hybrids formed by pillaring layered inorganic materials with organic molecules provide unique nanoporous surfaces surrounded by inorganic and organic moieties.<sup>2</sup> In general, the properties of inorganic–organic hybrids depend on their structures as well as their inorganic–organic junctions. Thus, the precise design of such hybrids is crucial for the development of desired functions.

Pillaring layered materials with organic molecules through covalent bonds is a rational approach for building well-ordered nanostructured materials with specific building units.<sup>5</sup> The size of the organic groups affects the interlayer gallery height, and the location and arrangement of reactive sites in layered materials define the lateral distance of immobilized organic moieties. Pillared layered metal phosphates/phosphonates were first introduced by Dines et al. in an effort to cross-link zirconium phosphate layers with rigid organo-

diphosphonates.<sup>6</sup> However, fully pillared zirconium phosphate has a crystalline structure with no porosity because of the closeness of adjacent phenylene pillars ( $\sim 5.3$  Å).<sup>7</sup> Thus, the introduction of spacer molecules such as  $-\text{O}_3\text{PH}$  groups is indispensable for producing porosities. The organic groups in those diphosphonates are easily designed,<sup>7</sup> but the inorganic structures are difficult to design in a controlled manner because most of the pillared layered metal phosphates/phosphonates are synthesized by dissolution–reprecipitation processes.<sup>8–11</sup> On the other hand, the topotactic phosphate/phosphonate exchange using  $\gamma$ -zirconium phosphate has been proposed, but the diversity of layered metal phosphates is limited.<sup>12–15</sup>

Two-dimensional (2D) layered silicates are versatile scaffolds for 3D silica nanostructures because of stable silicate structures and regular arrangements of Si–OH/Si–O<sup>−</sup> groups on their surfaces.<sup>16</sup> The typical examples are magadiite,<sup>17</sup> kenyaite,<sup>17</sup> MCM-22 (MWW),<sup>18</sup> RUB-15,<sup>19</sup> PREFER,<sup>20</sup> HLS,<sup>21</sup> AMH-3,<sup>22</sup> and M<sub>2</sub>Si<sub>2</sub>O<sub>5</sub> (M = H, Li, Na, K, Cs, Rb,

- (6) Dines, M. B.; Di Giacomo, P. M.; Callahan, K. P.; Griffith, P. C.; Lane, R. H.; Cooksey, R. E. In *Chemically Modified Surfaces in Catalysis and Electrocatalysis*; Miller, J. S., Ed.; ACS Symposium Series 192; American Chemical Society: Washington, DC, 1982; p 223.
- (7) Dines, M. B.; Cooksey, R. E.; Griffith, P. C.; Lane, R. H. *Inorg. Chem.* **1983**, *22*, 1003.
- (8) Alberti, G.; Costantino, U.; Marmottini, F.; Vivani, R.; Zappelli, P. *Angew. Chem., Int. Ed.* **1993**, *32*, 1357.
- (9) Clearfield, A. *Chem. Mater.* **1998**, *10*, 2801.
- (10) Clearfield, A.; Wang, Z. *J. Chem. Soc., Dalton Trans.* **2002**, 2937.
- (11) Mutin, P. H.; Guerrero, G.; Vioux, A. *J. Mater. Chem.* **2005**, *15*, 3761.
- (12) Yamanaka, S. *Inorg. Chem.* **1976**, *15*, 2811.
- (13) Brunet, E.; Huelva, M.; Rodríguez-Ubis, J. C. *Tetrahedron Lett.* **1994**, *35*, 8697.
- (14) Alberti, G.; Giontella, E.; Murcia-Mascarós, S. *Inorg. Chem.* **1997**, *36*, 2844.
- (15) Brunet, E.; de la Mata, M. J.; Alhendawi, H. M. H.; Cerro, C.; Alonso, M.; Juanes, O.; Rodríguez-Ubis, J. C. *Chem. Mater.* **2005**, *17*, 1424.

\* To whom correspondence should be addressed. Phone & Fax: 81-3-5286-3199. E-mail: kuroda@waseda.jp.

<sup>†</sup> Department of Applied Chemistry, Waseda University.

<sup>‡</sup> Kagami Memorial Laboratory for Materials Science and Technology, Waseda University.

<sup>§</sup> CREST, Japan Science and Technology Agency (JST).

- (1) Judeinstein, P.; Sanchez, C. *J. Mater. Chem.* **1996**, *6*, 511.
- (2) Clearfield, A. *Curr. Opin. Solid State Mater. Sci.* **2002**, *6*, 495.
- (3) Eddaoudi, M.; Kim, J.; Rosi, N.; Vodak, D.; Wachter, J.; O’Keeffe, M.; Yaghi, O. *Science* **2002**, *295*, 469.
- (4) Forster, P. M.; Cheetham, A. K. *Top. Catal.* **2003**, *24*, 1479.
- (5) Alberti, G.; Casciola, M.; Costantino, U.; Vivandi, R. *Adv. Mater.* **1996**, *8*, 291.

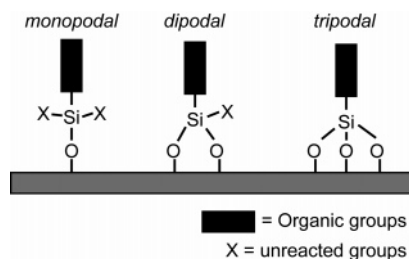


**Figure 1.** Different bonding modes of organosilyl units to a silicate surface.

and their mixture).<sup>23–27</sup> Various methodologies have been developed, and one of them is interlayer condensation with pillaring monomeric and/or oligomeric species. However, the regularities of the interlayer surfaces are not well-retained because of random polymerization of those species.<sup>28–30</sup> Recently, we have reported new crystalline silica structures by controlled silylation of layered silicates using dialkoxydichlorosilanes or alkoxytrichlorosilanes.<sup>31,32</sup> Layered octosilicate (known as ilerite and RUB-18) is a rational scaffold for controlled silylation because its crystalline structure imposes a constrained geometry to preferentially induce a dipodal reaction of one silylating agent with two confronting Si–OH/Si–O<sup>−</sup> groups (Figure 1).<sup>33</sup> Quite interestingly, the dipodal reaction leaves a functional group as a residual site at the inorganic–organic interface. The residual groups are crucial for the affinity of interlayer nanospaces, which shows different adsorption behaviors of polar molecules.<sup>34–36</sup>

The objective of this work is to design new microporous inorganic–organic hybrids using the silylation followed by crosslinking of layered octosilicate with 1,4-bis(trichlorosilyl)benzene or 1,4-bis(methyldichlorosilyl)benzene. Inorganic–organic nanohybrids derived from  $\alpha,\omega$ -organo-bis-silanetriols or  $\alpha,\omega$ -organo-bis-silanedioles are of great interest because of their chemical nature.<sup>37–39</sup> However, porous materials did not show any crystallinity at a molecular level, although nonporous materials showed a crystallinity attributed to the stacking of organic species. Though a biphenylene-pillared layered octosilicate with 4,4′-bis(trialkoxysilyl)biphenylene was reported by Ishii et al.,<sup>40</sup> its structure exhibited a low crystallinity because of the low reactivity of alkoxysilyl groups. In contrast, silylation using Si–Cl groups exhibits a high reactivity to the Si–OH groups, reflecting the original silicate structure in the silylated samples. Furthermore, we also focus on the dipodal reaction, which makes it possible to leave one site of the silylating agents. The remaining site is utilizable by the selection of appropriate silylating agents, and the method reported here should contribute to the development of multifunctional zeolitic structures.

## Experimental Section

**Materials.** All the synthetic reactions of the silylating agents were carried out under N<sub>2</sub> using a vacuum line and Schlenk technique. Solvents were dried and distilled just before use.

1,4-Bis(trichlorosilyl)benzene (**1**) was synthesized by the reaction of a Grignard reagent of 1,4-dibromobenzene (Tokyo Kasei Co.) with tetrachlorosilane (Tokyo Kasei Co.). A mixture of 1,4-dibromobenzene and magnesium chips in dry THF with a Mg:1,4-dibromobenzene ratio of 2 was heated at 70 °C for 24 h. The white suspension was added to an excess solution of tetrachlorosilane in THF at −10 °C. The suspension was then stirred for 24 h at room temperature. After the filtration of the suspension, the filtrate was evaporated under a vacuum and a crude oil was doubly distilled under a vacuum (bp 80 °C, 1 × 10<sup>−1</sup> Torr) to afford 1,4-bis(trichlorosilyl)benzene as a clear solid: <sup>1</sup>H NMR (500 MHz, CDCl<sub>3</sub>)  $\delta$  7.9; <sup>13</sup>C NMR (125.7 MHz, CDCl<sub>3</sub>)  $\delta$  132.8, 136.2; <sup>29</sup>Si NMR (99.3 MHz, CDCl<sub>3</sub>)  $\delta$  −1.7.

1,4-Bis(dichloromethylsilyl)benzene (**2**) was prepared by following the same reaction starting from 1,4-dibromobenzene and trichloromethylsilane (Tokyo Kasei Co.). After a usual workup, the compound was obtained as a clear solution by vacuum distillation (bp 60 °C, 1 × 10<sup>−1</sup> Torr): <sup>1</sup>H NMR (500 MHz, CDCl<sub>3</sub>)  $\delta$  1.0, 7.8; <sup>13</sup>C NMR (125.7 MHz, CDCl<sub>3</sub>)  $\delta$  5.4, 132.7, 137.2; <sup>29</sup>Si NMR (99.3 MHz, CDCl<sub>3</sub>)  $\delta$  18.2.

Na-octosilicate (Na-Oct; Na<sub>8</sub>[Si<sub>32</sub>O<sub>64</sub>(OH)<sub>8</sub>·32H<sub>2</sub>O]) was prepared according to the literature.<sup>29</sup> SiO<sub>2</sub> (special grade, Wako Chemicals), NaOH, and distilled water were mixed in a 4:1:25.8 SiO<sub>2</sub>:Na<sub>2</sub>O:H<sub>2</sub>O ratio. The mixture was treated at 100 °C for 4 weeks in a sealed Teflon vessel. Hexadecyltrimethylammonium-octosilicate (C<sub>16</sub>TMA-Oct), prepared by the ion-exchange reaction of Na-Oct with hexadecyltrimethylammonium chloride (C<sub>16</sub>H<sub>33</sub>N(CH<sub>3</sub>)<sub>3</sub>Cl, C<sub>16</sub>TMACl; Tokyo Kasei Co.),<sup>21</sup> was used as an intermediate. Na-Oct (12 g) was dispersed in an aqueous solution of C<sub>16</sub>TMACl (0.1 mol/L, 400 mL). The mixture was stirred for 24 h

- (16) Schwieger, W.; Lagaly, G. Alkali Silicates and Crystalline Silicic Acids. In *Handbook of Layered Materials*; Auerbach, S. M., Carrado, K. A., Dutta, P. K., Eds.; Marcel Dekker: New York, 2004; Chapter 11, pp 541–630.
- (17) Eugster, H. P. *Science* **1967**, *157*, 1177.
- (18) Leonowicz, M. E.; Lawton, J. A.; Lawton, S. L.; Rubin, M. K. *Science* **1994**, *264*, 1910.
- (19) Oberhagemann, U.; Bayat, P.; Marler, B.; Gies, H.; Rius, J. *Angew. Chem., Int. Ed.* **1996**, *35*, 2869.
- (20) Schreyeck, L.; Caullet, P.; Mougengel, J. C.; Guth, J. L.; Marler, B. *Microporous Mesoporous Mater.* **1996**, *6*, 259.
- (21) Akiyama, Y.; Mizukami, F.; Kiyozumi, Y.; Maeda, K.; Izutsu, H.; Sakaguchi, K. *Angew. Chem., Int. Ed.* **1999**, *38*, 1420.
- (22) Jeong, H. K.; Nair, S.; Vogt, T.; Dickinson, L. C.; Tsapatsis, M. *Nat. Mater.* **2003**, *2*, 53.
- (23) Kahlenberg, V.; Dörsam, G.; Wendschuh-Josties, M.; Fischer, R. X.; *J. Solid State Chem.* **1999**, *146*, 380.
- (24) Ai, X.; Deng, F.; Jinxiang, D.; Chen, L.; Ye, C. *J. Phys. Chem. B* **2002**, *106*, 9237.
- (25) de Jong, B. H. W. S.; Slaats, P. G. G.; Super, H. T. J.; Veldman, N.; Spek, A. L. *J. Non-Cryst. Solids* **1994**, *176*, 164.
- (26) Le Bihan, M. T.; Kalt, A.; Wey, R. *Bull. Soc. Fr. Mineral. Cristallogr.* **1971**, *94*, 15.
- (27) Rakic, S.; Kahlenberg, V.; Schmidt, B. C. Z. *Krystallogr.* **2003**, *218*, 413.
- (28) Cool, P.; Vansant, E. F. Pillared Porous Clay Heterostructures. In *Handbook of Layered Materials*; Auerbach, S. M., Carrado, K. A., Dutta, P. K., Eds.; Marcel Dekker: New York, 2004; Chapter 6, pp 261–311.
- (29) Kosuge, K.; Tsunashima, A. *J. Chem. Soc., Chem. Commun.* **1995**, 2427.
- (30) Galarneau, A.; Barodawalla, A.; Pinnavaia, T. J. *Nature* **1995**, *374*, 529.
- (31) Mochizuki, D.; Shimojima, A.; Kuroda, K. *J. Am. Chem. Soc.* **2002**, *124*, 12082.
- (32) Mochizuki, D.; Shimojima, A.; Imagawa, T.; Kuroda, K. *J. Am. Chem. Soc.* **2005**, *127*, 7183.
- (33) Vortmann, S.; Rius, J.; Siegmann, S.; Gies, H. *J. Phys. Chem. B* **1997**, *101*, 1292.
- (34) Ogawa, M.; Okutomo, S.; Kuroda, K. *J. Am. Chem. Soc.* **1998**, *120*, 7361.
- (35) Fujita, I.; Kuroda, K.; Ogawa, M. *Chem. Mater.* **2003**, *15*, 3134.
- (36) Fujita, I.; Kuroda, K.; Ogawa, M. *Chem. Mater.* **2005**, *17*, 3718.

- (37) Cerveau, G.; Chappellet, S.; Corriu, R. J. P.; Dabiens, B. *J. Organomet. Chem.* **2001**, *626*, 92.
- (38) Cerveau, G.; Corriu, R. J. P. *Coord. Chem. Rev.* **1998**, *180*, 1051.
- (39) Loy, D. A.; Shea, K. J. *Chem. Rev.* **1995**, *95*, 1431.
- (40) Ishii, R.; Shinohara, Y. *J. Mater. Chem.* **2005**, *15*, 551.

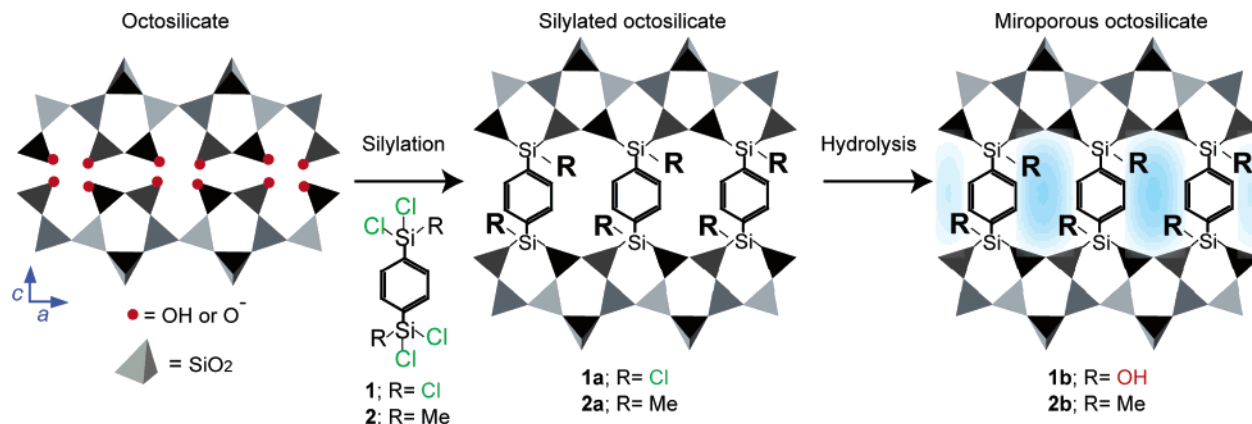


Figure 2. Silylation of octosilicate with 1,4-bis(trichloro- and dichloromethyl-silyl)benzenes.

at room temperature and then centrifuged to remove the supernatant. This procedure was repeated three times. The resulting slurry was washed with water and air-dried at room temperature.

**Silylation.** Silylation of layered octosilicate was performed according to the literature.<sup>41</sup>  $C_{16}$ TMA-Oct (1.5 g) dispersed in dehydrated dichloromethane (30 mL) and dehydrated pyridine (10 mL) was mixed with an excess amount of the silylating agents. The mixture was stirred for 1 day at room temperature under a  $N_2$  atmosphere. The solid products were filtered and washed with dichloromethane to remove unreacted silylating reagents, pyridine hydrochloride, and de-intercalated  $C_{16}$ TMACl. The resulting products were dried in vacuo to yield **1a** and **2a** (Figure 2). The samples were then washed with a mixture of acetone and an aqueous 1 M HCl solution for the removal of  $C_{16}$ TMA cations and the conversion of remaining Si–Cl groups to Si–OH groups and dried under a vacuum.

**Adsorption of Phenol.** Adsorption of phenol by the derivatives **1b** and **2b** (Figure 2) from an aqueous solution was conducted according to the literature.<sup>42</sup> A silylated sample (20 mg) was dispersed in an aqueous solution of phenol (30 mL) for 1 day at 25 °C. After the suspension was centrifuged, the concentration of phenol in the resulting supernatant was measured by UV absorption spectroscopy (absorption  $\lambda_{\max} = 269$  nm). The adsorption amount of phenol was calculated by the difference in concentration between the original solution and the resulting one.

**Analysis.** Powder X-ray diffraction (XRD) measurements were performed on a Rigaku Rint 2000 powder diffractometer with monochromated Cu K $\alpha$  radiation ( $\lambda = 1.5405$  Å). Thermogravimetry (TG) was carried out with a Rigaku Thermo Plus2 instrument under a dry air flow at a heating rate of 10 °C  $min^{-1}$ , and the amount of  $SiO_2$  fraction in the products was determined by the residual weight after heating to 900 °C. The amounts of organic constituents were determined by CHN analysis (Perkin-Elmer PE-2400). Solid-state  $^{29}Si$  MAS NMR spectra were recorded on a JEOL JNM-CMX-400 spectrometer at a resonance frequency of 79.42 MHz. We confirmed that the signals were fully relaxed under a recycle delay of 400 s with a 45° pulse so that quantitative analysis was possible. Samples were put into 7.5 mm (or 5 mm) zirconia rotors and spun at 5 kHz. Solid-state  $^{13}C$  CP/MAS NMR spectra were recorded on the same spectrometer at a resonance frequency of 100.40 MHz and a recycle delay of 5 s. The  $^{29}Si$  and  $^{13}C$  chemical shifts were referenced to tetramethylsilane at 0 ppm. Nitrogen adsorption measurements were carried out on a Quantachrome Autosorb-1MP. Prior to the adsorption measurements, samples were outgassed at 120 °C for 3 h. BET surface areas were calculated from the

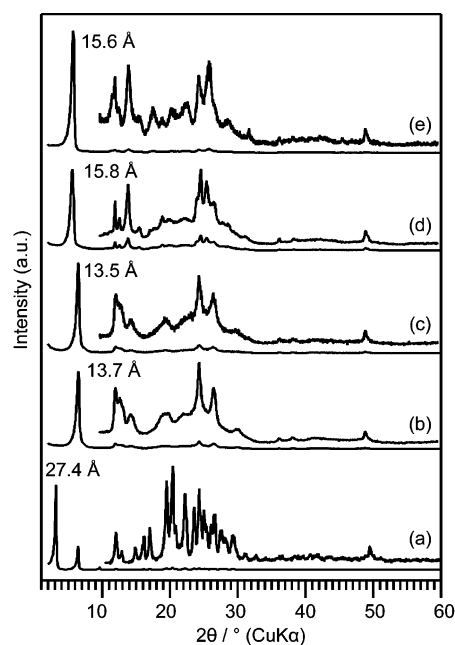


Figure 3. XRD patterns of (a)  $C_{16}$ TMA-Oct, (b) **1a**, (c) **1b**, (d) **2a**, and (e) **2b**.

adsorption data in the relative pressure range around 0.1. The micropore volume was calculated by  $t$ -plot method. Pore size distribution was calculated from adsorption branches using the Horváth–Kawazoe method (slit pore geometry).<sup>43</sup> Water vapor adsorption isotherms at 25 °C were collected on a Belsorp 18 (Bel Japan, Inc.). Samples were outgassed at 120 °C for 3 h prior to the measurements. The scanning electron microscopic (SEM) images were obtained with a JEOL JSM-5500LV microscope at an accelerating voltage of 25 kV. UV absorption spectra were obtained on a Shimadzu UV-2500PC spectrometer. Structurally optimized calculation was performed with an Accelrys Discover software by using the COMPASS force field. The void occupancies of the optimized structures were calculated using a Material Studio software with packaging balls of 4 Å.

## Results and Discussion

**Synthesis of Silylated Derivatives.** The XRD patterns of the intermediate and the silylated samples are shown in Figure 3. The silylated samples of **1b** and **2b** showed new peaks with repeat distances of 13.5 and 15.6 Å, respectively,

(41) Endo, K.; Sugahara, Y.; Kuroda, K. *Bull. Chem. Soc. Jpn.* **1994**, *67*, 3352.

(42) Okada, T.; Watanabe, Y.; Ogawa, M. *J. Mater. Chem.* **2005**, *15*, 987.

(43) Horváth, G.; Kawazoe, K. *J. Chem. Eng. Jpn.* **1983**, *16*, 470.

**Table 1.** Amount of Phenylene Groups of the Silylated Samples

	mass % C	mass % N	% SiO <sub>2</sub>	amount of phenylene groups/ (SiOH + SiO <sup>-</sup> ) <sup>a</sup> (mmol/g)	amount of phenylene groups (A) mmol/g
C <sub>16</sub> TMA-Oct	38.1	2.3	45.2		
<b>1b</b>	11.6	0.0	85.1	0.25	1.61
<b>2b</b>	14.9	0.0	84.5	0.25	1.55

<sup>a</sup> Evaluated by <sup>29</sup>Si MAS NMR and thermogravimetry.

which is slightly decreased from **1a** and **2a** (13.7 and 15.8 Å, respectively). The heights of the interior region (gallery height) were estimated to be 6.1 and 8.2 Å for **1b** and **2b**, respectively, by subtracting the *d*-spacing of protonated octosilicate (7.4 Å) from the observed *d*-values. The interior heights are slightly shorter than the molecular length of the silylating agents (8.6 Å), suggesting that the 1,4-disilylphenyl groups obliquely bridged adjacent layers to form pillared structures. The complete removal of C<sub>16</sub>TMA cations was confirmed by the absence of nitrogen content in the silylated derivatives (Table 1). The remaining carbon portions in the silylated derivatives correspond to phenylene groups, as revealed by <sup>13</sup>C CP/MAS NMR (see the Supporting Information, Figure S1). These data demonstrate the attachments of the silyl groups onto the interlayer surface. The number of attached phenylene groups in **1b** and **2b** was estimated to be 0.25 per Si–OH/Si–O<sup>-</sup> unit, as determined by the chemical compositions. These values are half of those reported for the alkoxy-silylated products,<sup>32</sup> implying that both silyl groups of one molecule react with the Si–OH/Si–O<sup>-</sup> units on the interlayer surfaces. In the higher diffraction angle of the XRD patterns of the silylated derivatives, many peaks attributed to the crystalline nature of the silicate are observed. All of the (00*l*) reflections are broadened, suggesting that the atomic arrangement within the silicate layers is well-ordered but the stacking along the *c*-axis is less-ordered. This less-ordered stacking was also observed for the topotactic conversion of octosilicate.<sup>44</sup> In addition, the peaks at around 49°, which are assigned to the intralayer ordering, also indicate well-ordered structures within the silicate layer. The morphologies of the silylated samples did not change from that of the intermediate (see the Supporting Information, Figure S2).

The <sup>29</sup>Si MAS NMR spectra of the products are shown in Figure 4, and the relative intensities of the signals are shown in Tables 2 and 3. The spectrum of octosilicate shows two signals at -100 and -110 ppm, corresponding to Q<sup>3</sup> and Q<sup>4</sup> sites, respectively, with an intensity ratio (Q<sup>3</sup>:Q<sup>4</sup>) of 1. The spectrum of the sample before the treatment with a mixture of acetone/HCl aq. (**1a**) shows a new signal at -52 ppm. This signal can be ascribed to the dipodally grafted silyl groups (*Si*(OSi)<sub>2</sub>C1R) because the signal is shifted downfield from the T<sup>2</sup> site (*Si*(OSi)<sub>2</sub>(OH)R) of phenyl-silylated samples (typically appears at -65 ppm<sup>32</sup>). In particular, the signal due to the dipodal grafting was shifted to the T<sup>2</sup> site after the acid treatment (Figure 4c). The signal at -1 ppm is also observed in the spectrum of **1a**, indicating the presence of unreacted silyl groups (RSiCl<sub>3</sub>), although the relative intensity is very small (~10%) compared to those

of the dipodally grafted groups. Such unreacted silyl groups can be assigned to a silyl group located opposite to the grafted silyl group in one silylating molecule, because totally unreacted silylating molecules should be completely removed during the washing process. The spectrum of **2a** shows two signals due to the silyl groups, corresponding to D<sup>2</sup> (-27 ppm) and unreacted silyl groups (18 ppm). The intensities attributed to the silylating groups are estimated to be 0.5 per Si–OH (or Si–O<sup>-</sup>) group of octosilicate. This value is approximately twice that of phenylene groups (0.25), which is in good agreement with the number of attached silyl groups per Si–OH (or Si–O<sup>-</sup>) evaluated by the TG and elemental analysis. The relative intensity of the Q<sup>3</sup> signal of C<sub>16</sub>TMA-Oct decreased to ca. 0.1 after silylation, indicating that 90% of reactive sites are reacted. The dipodal grafting of silyl groups onto layered octosilicate is confirmed by the value of 2.1 in the ratio of increments of the Q<sup>4</sup> signal to the amount of silylated sites (*Si*(OSi)<sub>2</sub>C1R and *Si*(OSi)<sub>2</sub>R<sub>2</sub>).

After the treatment with a mixture of acetone/HCl aq., the spectra of the silylated samples show the new signals due to the T<sup>1</sup> (*Si*(OSi)(OH)<sub>2</sub>R, -60 ppm) T<sup>2</sup> (*Si*(OSi)<sub>2</sub>(OH)R, -67 ppm), and T<sup>3</sup> (*Si*(OSi)<sub>3</sub>R, -76 ppm) sites for **1b**, and D<sup>1</sup> (*Si*(OSi)(OH)R<sub>2</sub>, -17 ppm) for **2b**. The new T<sup>1</sup> and D<sup>1</sup> sites were presumably generated by the hydrolysis and condensation of the unreacted silyl groups, because the intensities of these sites were comparable to those of the unreacted sites (SiCl<sub>3</sub>R or SiCl<sub>2</sub>R<sub>2</sub>) in **1a** and **2a**. Likewise, the new T<sup>3</sup> site appeared by the condensation of the *Si*(OSi)<sub>2</sub>C1R site with unreacted silyl groups. The total relative intensities of these signals are approximately equal to that of the silyl groups in **1a**. The presence of unreacted silyl groups means that the silylating agents incompletely bridge between silicate layers. This is attributed to the overloading of silyl groups because

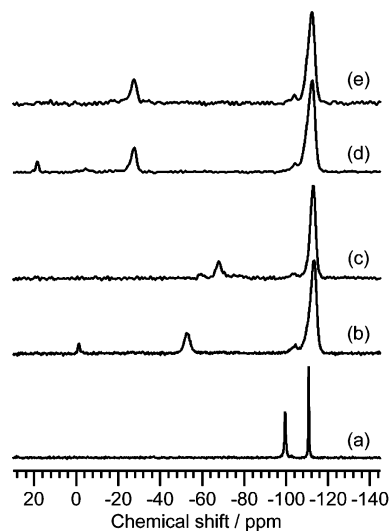


**Figure 4.** <sup>29</sup>Si MAS NMR spectra of (a) C<sub>16</sub>TMA-Oct, (b) **1a**, (c) **1b**, (d) **2a**, and (e) **2b**.

(44) Marler, B.; Stroter N.; Gies, H. *Microporous Mesoporous Mater.* **2005**, *83*, 201.

Table 2. Relative Intensities in the  $^{29}\text{Si}$  MAS NMR Spectra of the Samples Silylated with 1

Site								$\frac{Q^4-1}{I}$
Chemical shift (ppm)	-1	-52	-60	-67	-76	-100	-110	
C <sub>16</sub> TMA-Oct						1.00	1.00	-
<b>1a</b>	0.06	0.39				0.15	1.85	2.1
<b>1b</b>			0.07	0.38	0.10	0.12	1.88	-

Table 3. Relative Intensities in the  $^{29}\text{Si}$  MAS NMR Spectra of the Samples Silylated with 2

Site					$\frac{Q^4-1}{D^2}$
Chemical shift (ppm)	18	-17	-27	-100	-110
<b>2a</b>	0.06		0.38	0.17	1.83
<b>2b</b>		0.04	0.46	0.13	1.87

<sup>a</sup> The intensity of D<sup>2</sup> for **2b** includes that of the site formed by the condensation of the unreacted silyl groups (Ph-SiMeCl<sub>2</sub>). Thus, it is not so meaningful to calculate the ratio of (Q<sup>4</sup>-1)/D<sup>2</sup>.

of the wider interlayer gallery height of C<sub>16</sub>TMA-Oct. However, the ratio of unreacted sites is relatively low, probably because of the contribution of the steric hindrance of phenylene groups.

**Microporosity of the Silylated Samples.** The silylated samples **1b** and **2b** showed clear Type I adsorption/desorption isotherms (Figure 5), characteristic of microporous materials, with BET surface areas of 520 and 470 m<sup>2</sup>/g, respectively (Table 4). These values are similar to that of biphenylene pillared octosilicate (616 m<sup>2</sup>/g).<sup>40</sup> The pore size distribution curves of these samples showed the presence of micropores with diameters centered at ca. 5 Å (Figure 5). The diameter is quite reasonable if the distance between the phenylene groups is considered, because the repeating distance of phenylene groups is estimated to be 7.4 Å on the basis of the arrangement of Si–OH groups in octosilicate, and the thickness of phenylene groups is estimated to be ~2 Å. The micropores of **1b** and **2b** are formed by bridging the silicate layers with enough distances between pillars, whereas Ishii et al. assumed that the microporosity of biphenylene pillared octosilicate can be derived from the extraction of *n*-hexylamine as co-intercalated guest species.<sup>40</sup> This difference may occur because of the different reactivities of the silylating agents. The reaction of Si–Cl groups with Si–OH groups induces the removal of surfactants because of the generation of HCl as byproduct,<sup>34</sup> although that of Si–OR groups does not remove organoammonium cations. Therefore, the formation of microporosity reported here is completely different from that of the biphenylene pillared octosilicate. The microporous structures are thermally stable to 500 °C without any loss of the phenylene groups (see the Supporting Information, Figure S3).

To estimate the hydrophilicity of the microporous surface, we have shown the water adsorption isotherms of two silylated samples in Figure 6. The isotherm of **1b** exhibits a

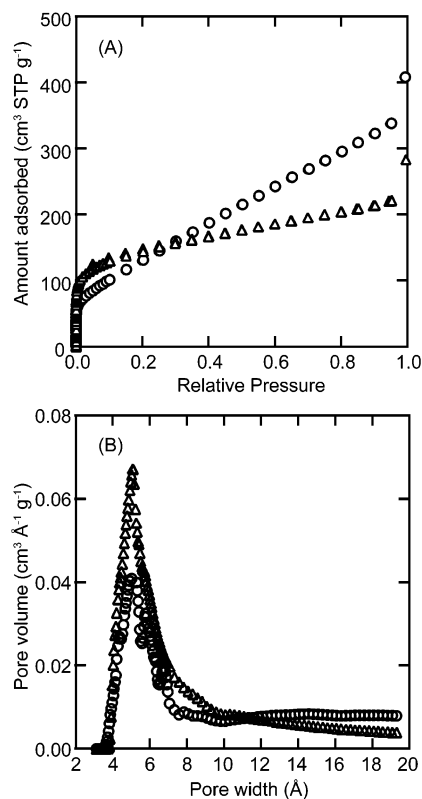


**Figure 5.** (A) Nitrogen adsorption isotherms and (B) pore size distributions calculated by the HK method. Circles and triangles correspond to **1b** and **2b**, respectively.

larger amount of adsorbed water than that of **2b**, which reveals that **1b** has a hydrophilic pore surface. It is well-known that the hydrophilicity of a surface depends on the number of Si–OH groups. Actually, **1b** has a large amount of Si–OH groups because of the presence of transformed

Table 4. Porosities of the Samples and Adsorption Data of Phenol

	N <sub>2</sub> adsorption		phenol adsorption				
	surface area (m <sup>2</sup> /g)	pore volume (B) (cm <sup>3</sup> /g)	maximum adsorbed amount (C) (mmol/g)	correlation factor <i>r</i> <sup>2</sup>	volume of adsorbed phenol (D) (cm <sup>3</sup> /g)	volume ratio of adsorbed phenol (D)/pore (B)	molar ratio of adsorbed phenol (C)/phenylene groups (A) <sup>a</sup>
<b>1b</b>	470	0.24	0.165	0.992	0.016	0.07	0.10
<b>2b</b>	520	0.27	0.857	0.995	0.084	0.31	0.55

<sup>a</sup> Amounts of phenylene groups (A) are shown in Table 1.

OH groups after the dipodal reaction, but **2b** has a small amount of Si–OH groups of unreacted interlayer surface silanol groups. However, the amount of adsorbed water in **1b** at saturated pressure (~6 mmol/g) is small, if compared with the microporosity of 0.24 cm<sup>3</sup>/g (15mmol/g). This can be attributed to the presence of both Si–OH groups and phenylene groups in the micropores.

The phenol adsorption isotherms for the silylated samples exhibited L type adsorption (Figure 7). The maximum amounts of adsorbed phenol in the samples **1b** and **2b** were estimated to be 0.165 and 0.857 mmol/g, respectively (Table 4). It is known that layered silicates silylated with alkyl-trichlorosilanes adsorb *n*-alcohols in the interlayer space rather than the products silylated with alkyl-dimethylchlorosilanes because of the hydrogen-bonding of OH groups between alcohols and Si–OH groups.<sup>34–36</sup> In contrast, the phenylene pillared octosilicates showed a different behavior from the alkylsilylated layered silicates, possibly because of differences in the adsorption mechanism. The adsorbed amount in **2b** is larger or similar to that observed for other

organically modified clay materials,<sup>42</sup> indicating that the phenylene pillared octosilicate acts as an effective adsorbent for phenol. Molar ratios of adsorbed phenols to phenylene groups (0.55) are higher than the volume ratios of adsorbed volumes to micropores (0.31), suggesting that the adsorbed phenol preferentially interacts with phenylene groups (Table 4). However, the amount of adsorbed phenol does not reach the value of full interaction with phenylene groups, probably because of the hindrance of methyl groups.

**Ideal Structures of the Silylated Samples.** We propose ideal structures of the silylated samples using the data described above. On the basis of the <sup>29</sup>Si MAS NMR spectra, two different structures for the attached silyl groups can be proposed on the assumption of the unchanged crystal structure of octosilicate. One model shows that one bis(trichlorosilyl)benzene molecule perpendicularly bridges between adjacent layers, resulting in pillaring of the interlayer space. The other model involves the parallel arrangement of the phenylene groups by reaction with the Si–OH sites on one interlayer surface. In the present study, we can choose the model of interlayer pillaring because the dipodal reaction of silyl groups leads to perpendicular alignments of the phenylene groups because of tetrahedral coordination of Si species. It is impossible to determine the crystal structures of the products because there are a couple of possibilities on the crystal systems (tetragonal, monoclinic, or orthorhombic cell) caused by several possible alignments of Si–Me/Si–OH groups (see the Supporting Information, Figure S4). The crystal systems cannot be determined by the XRD pattern fitting, because their proposed structures are very similar and the structures are probably a mixture of these structures. One of the ideal structures simulated with Discover software is shown in Figure 8. The micropores are surrounded by phenylene groups and silicate layers with the functional groups because of the unreacted sites. The pore volumes of these structures calculated by the Material Studio software are estimated to be 0.21 and 0.26 cm<sup>3</sup>/g for **1b** and **2b**, respectively. These values are in good agreement with the experimental values calculated from the N<sub>2</sub> adsorption data (0.24 and 0.27 cm<sup>3</sup>/g for **1b** and **2b**, respectively), supporting the reliability of these models.

On the other hand, the basal-spacings differed between **1b** and **2b** (the difference is 2.1 Å). According to previous reports,<sup>35</sup> the basal spacings of silylated derivatives of magadiite correspond to the degree of silylation. However, the amounts of silyl groups in both of the silylated samples are almost equivalent here. Thus, the difference is presumably caused by the alignment of the phenylene groups. Moreover, the alignment of the phenylene groups is probably changed by the difference in the numbers of Si–Cl groups in one

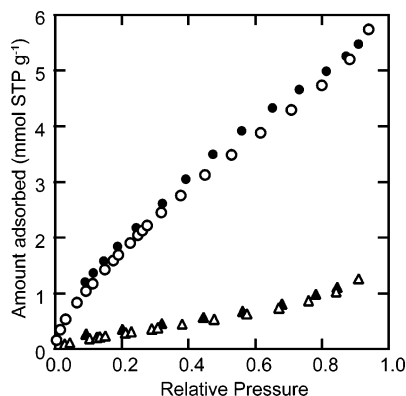


Figure 6. Water adsorption /desorption isotherms of **1b** (circles) and **2b** (triangles).

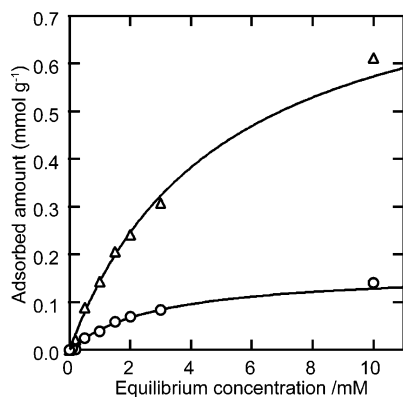
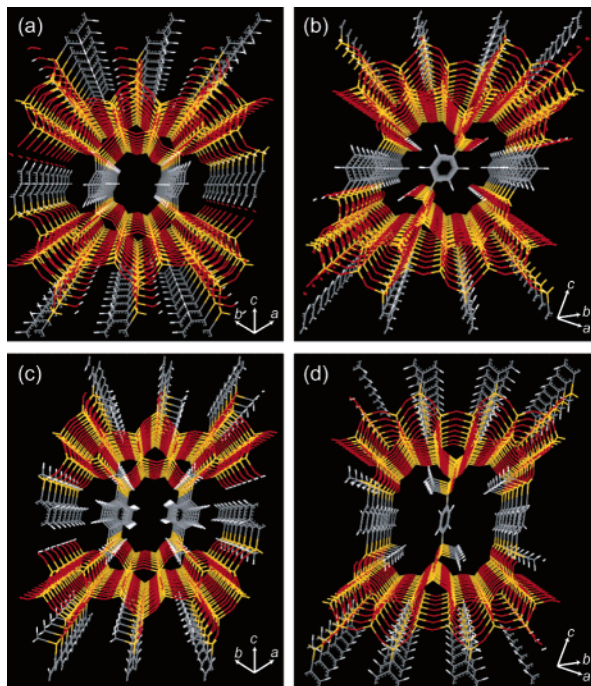


Figure 7. Adsorption isotherms of phenol on **1b** (circles) and **2b** (triangles).



**Figure 8.** Ideal structural models of **1b** and **2b** as simulated using Discover. Perspective views of **1b** along (a) [110] and (b) [110] and **2b** along (c) [110] and (d) [110] directions.

silyl groups. The dipodal grafting is proceeded not by simultaneous reaction but by two consecutive reactions, which is proved by the monopodal grafting of trichlorosilanes with a short-alkyl chain.<sup>46</sup> Thus, one Si–Cl group in one silyl group reacts with one Si–OH site, and another Si–Cl group in the silyl group subsequently reacts with the other confronting Si–OH site. Here, a large difference should occur between trichlorosilyl and dichlorosilyl groups because of the different selectivities of the reactive sites. In other words, dichlorosilyl groups are forced to take one alignment of phenylene groups because the only remaining Si–Cl group must react with the confronting silanol group on the interlayer surface,

(45) *International Table for Crystallography, Vol. A*; Hahn, T., Ed.; D. Riedel Publishing Co.: Dordrecht, The Netherlands, 1983.

(46) When octosilicate reacts with dibutoxydichlorosilane, the silyl groups are partially grafted with a monopodal mode (see ref. 20) because of a little steric hindrance of the alkyl groups. On the basis of this result, it is clear that, in the first stage, one chlorosilyl group of the dichlorosilyl groups first reacts with a Si–OH group and then the other chlorosilyl group reacts with another Si–OH group.

whereas the trichlorosilyl groups may be able to take a more liable alignment of phenylene groups because one of the two remaining Si–Cl groups can react to form a dipodal grafting. Therefore, the sample silylated with trichlorosilanes is expected to form a smaller basal spacing to attain a more stable conformation.

### Conclusions

Inorganic–organic microporous materials are prepared by interlayer silylation and pillaring of layered octosilicate with 1,4-bis(trichlorosilyl)benzene and 1,4-bis(dichloromethylsilyl)benzene in a controlled manner. The dipodal reaction of the silyl groups onto the silicate leaves functional sites of hydroxysilyl and methylsilyl groups that do not react with the interlayer surfaces. These unreacted sites largely affect the microporous surface properties. The microporosity of the inorganic–organic hybrids can easily be controlled by the design of silylating agents. This method can be extended to other layered silicates such as magadiite and kenyaite with different interlayer surface structures and layer thicknesses,<sup>47</sup> which is promising for future nanoporous materials design. Moreover, crosslinking phenylene groups can be modified with sulfonation and bromination, indicating the prospective formation of well-designed bifunctional microporous hybrids.

**Acknowledgment.** We thank Dr. A. Shimojima, Professor Y. Sugahara, and Professor M. Ogawa (Waseda University) for helpful discussion. The work was partially supported by Grants-in-Aids for Center of Excellence (COE) Research “Molecular Nanoengineering”, the 21st Century COE Program “Practical Nanochemistry”, and Encouraging Development Strategic Research Centers Program “Establishment of Consolidated Research Institute for Advanced Science and Medical Care”, MEXT, Japan. This work is also supported by the A3 Foresight Program “Synthesis and Structural Resolution of Novel Mesoporous Materials” from the Japan Society for the Promotion of Science (JSPS). D.M. is grateful for financial support by a Grant-in-Aid for JSPS Fellows from MEXT.

**Supporting Information Available:** C-13 CP/MAS NMR spectra of **1a** and **1b**; SEM images of C<sub>16</sub>TMA-Oct and **1b**; TG curves of **1b** and **2b**; and proposed structures of **2b** (PDF). This material is available free of charge via the Internet at <http://www.acs.org>.

CM061357Q

(47) Mochizuki, D.; Kuroda, K. *New J. Chem.* **2006**, *30*, 277.